

Measurement of the Ratio of Branching Fractions $\mathcal{B}(B^\pm \rightarrow J/\psi\pi^\pm)/\mathcal{B}(B^\pm \rightarrow J/\psi K^\pm)$

A. Abulencia,²⁴ J. Adelman,¹³ T. Affolder,¹⁰ T. Akimoto,⁵⁶ M.G. Albrow,¹⁷ D. Ambrose,¹⁷ S. Amerio,⁴⁴ D. Amidei,³⁵ A. Anastassov,⁵³ K. Anikeev,¹⁷ A. Annovi,¹⁹ J. Antos,¹⁴ M. Aoki,⁵⁶ G. Apollinari,¹⁷ J.-F. Arguin,³⁴ T. Arisawa,⁵⁸ A. Artikov,¹⁵ W. Ashmanskas,¹⁷ A. Attal,⁸ F. Azfar,⁴³ P. Azzi-Bacchetta,⁴⁴ P. Azzurri,⁴⁷ N. Bacchetta,⁴⁴ W. Badgett,¹⁷ A. Barbaro-Galtieri,²⁹ V.E. Barnes,⁴⁹ B.A. Barnett,²⁵ S. Baroiant,⁷ V. Bartsch,³¹ G. Bauer,³³ F. Bedeschi,⁴⁷ S. Behari,²⁵ S. Belforte,⁵⁵ G. Bellettini,⁴⁷ J. Bellinger,⁶⁰ A. Belloni,³³ D. Benjamin,¹⁶ A. Beretvas,¹⁷ J. Beringer,²⁹ T. Berry,³⁰ A. Bhatti,⁵¹ M. Binkley,¹⁷ D. Bisello,⁴⁴ R.E. Blair,² C. Blocker,⁶ B. Blumenfeld,²⁵ A. Bocci,¹⁶ A. Bodek,⁵⁰ V. Boisvert,⁵⁰ G. Bolla,⁴⁹ A. Bolshov,³³ D. Bortoletto,⁴⁹ J. Boudreau,⁴⁸ A. Boveia,¹⁰ B. Brau,¹⁰ L. Brigliadori,⁵ C. Bromberg,³⁶ E. Brubaker,¹³ J. Budagov,¹⁵ H.S. Budd,⁵⁰ S. Budd,²⁴ S. Budroni,⁴⁷ K. Burkett,¹⁷ G. Busetto,⁴⁴ P. Bussey,²¹ K. L. Byrum,² S. Cabrera,¹⁶ M. Campanelli,²⁰ M. Campbell,³⁵ F. Canelli,¹⁷ A. Canepa,⁴⁹ S. Carillo,¹⁸ D. Carlsmith,⁶⁰ R. Carosi,⁴⁷ S. Carron,³⁴ M. Casarsa,⁵⁵ A. Castro,⁵ P. Catastini,⁴⁷ D. Cauz,⁵⁵ M. Cavalli-Sforza,³ A. Cerri,²⁹ L. Cerrito,⁴³ S.H. Chang,²⁸ Y.C. Chen,¹ M. Chertok,⁷ G. Chiarelli,⁴⁷ G. Chlachidze,¹⁵ F. Chlebana,¹⁷ I. Cho,²⁸ K. Cho,²⁸ D. Chokheli,¹⁵ J.P. Chou,²² G. Choudalakis,³³ S.H. Chuang,⁶⁰ K. Chung,¹² W.H. Chung,⁶⁰ Y.S. Chung,⁵⁰ M. Ciljak,⁴⁷ C.I. Ciobanu,²⁴ M.A. Ciocci,⁴⁷ A. Clark,²⁰ D. Clark,⁶ M. Coca,¹⁶ G. Compostella,⁴⁴ M.E. Convery,⁵¹ J. Conway,⁷ B. Cooper,³⁶ K. Copic,³⁵ M. Cordelli,¹⁹ G. Cortiana,⁴⁴ F. Crescioli,⁴⁷ C. Cuenca Almenar,⁷ J. Cuevas,¹¹ R. Culbertson,¹⁷ J.C. Cully,³⁵ D. Cyr,⁶⁰ S. DaRonco,⁴⁴ M. Datta,¹⁷ S. D'Auria,²¹ T. Davies,²¹ M. D'Onofrio,³ D. Dagenhart,⁶ P. de Barbaro,⁵⁰ S. De Cecco,⁵² A. Deisher,²⁹ G. De Lentdecker,⁵⁰ M. Dell'Orso,⁴⁷ F. Delli Paoli,⁴⁴ L. Demortier,⁵¹ J. Deng,¹⁶ M. Deninno,⁵ D. De Pedis,⁵² P.F. Derwent,¹⁷ G.P. Di Giovanni,⁴⁵ C. Dionisi,⁵² B. Di Ruzza,⁵⁵ J.R. Dittmann,⁴ P. DiTuro,⁵³ C. Dörr,²⁶ S. Donati,⁴⁷ M. Donega,²⁰ P. Dong,⁸ J. Donini,⁴⁴ T. Dorigo,⁴⁴ S. Dube,⁵³ J. Efron,⁴⁰ R. Erbacher,⁷ D. Errede,²⁴ S. Errede,²⁴ R. Eusebi,¹⁷ H.C. Fang,²⁹ S. Farrington,³⁰ I. Fedorko,⁴⁷ W.T. Fedorko,¹³ R.G. Feild,⁶¹ M. Feindt,²⁶ J.P. Fernandez,³² R. Field,¹⁸ G. Flanagan,⁴⁹ A. Foland,²² S. Forrester,⁷ G.W. Foster,¹⁷ M. Franklin,²² J.C. Freeman,²⁹ I. Furic,¹³ M. Gallinaro,⁵¹ J. Galyardt,¹² J.E. Garcia,⁴⁷ F. Garberon,¹⁰ A.F. Garfinkel,⁴⁹ C. Gay,⁶¹ H. Gerberich,²⁴ D. Gerdes,³⁵ S. Giagu,⁵² P. Giannetti,⁴⁷ A. Gibson,²⁹ K. Gibson,⁴⁸ J.L. Gimmell,⁵⁰ C. Ginsburg,¹⁷ N. Giokaris,¹⁵ M. Giordani,⁵⁵ P. Giromini,¹⁹ M. Giunta,⁴⁷ G. Giurgiu,¹² V. Glagolev,¹⁵ D. Glenzinski,¹⁷ M. Gold,³⁸ N. Goldschmidt,¹⁸ J. Goldstein,⁴³ A. Golossanov,¹⁷ G. Gomez,¹¹ G. Gomez-Ceballos,¹¹ M. Goncharov,⁵⁴ O. González,³² I. Gorelov,³⁸ A.T. Goshaw,¹⁶ K. Goulianos,⁵¹ A. Gresele,⁴⁴ M. Griffiths,³⁰ S. Grinstein,²² C. Grosso-Pilcher,¹³ R.C. Group,¹⁸ U. Grundler,²⁴ J. Guimaraes da Costa,²² Z. Gunay-Unalan,³⁶ C. Haber,²⁹ K. Hahn,³³ S.R. Hahn,¹⁷ E. Halkiadakis,⁵³ A. Hamilton,³⁴ B.-Y. Han,⁵⁰ J.Y. Han,⁵⁰ R. Handler,⁶⁰ F. Happacher,¹⁹ K. Hara,⁵⁶ M. Hare,⁵⁷ S. Harper,⁴³ R.F. Harr,⁵⁹ R.M. Harris,¹⁷ M. Hartz,⁴⁸ K. Hatakeyama,⁵¹ J. Hauser,⁸ A. Heijboer,⁴⁶ B. Heinemann,³⁰ J. Heinrich,⁴⁶ C. Henderson,³³ M. Herndon,⁶⁰ J. Heuser,²⁶ D. Hidas,¹⁶ C.S. Hill,¹⁰ D. Hirschbuehl,²⁶ A. Hocker,¹⁷ A. Holloway,²² S. Hou,¹ M. Houlden,³⁰ S.-C. Hsu,⁹ B.T. Huffman,⁴³ R.E. Hughes,⁴⁰ U. Husemann,⁶¹ J. Huston,³⁶ J. Incandela,¹⁰ G. Introzzi,⁴⁷ M. Iori,⁵² Y. Ishizawa,⁵⁶ A. Ivanov,⁷ B. Iyutin,³³ E. James,¹⁷ D. Jang,⁵³ B. Jayatilaka,³⁵ D. Jeans,⁵² H. Jensen,¹⁷ E.J. Jeon,²⁸ S. Jindariani,¹⁸ M. Jones,⁴⁹ K.K. Joo,²⁸ S.Y. Jun,¹² J.E. Jung,²⁸ T.R. Junk,²⁴ T. Kamon,⁵⁴ P.E. Karchin,⁵⁹ Y. Kato,⁴² Y. Kemp,²⁶ R. Kephart,¹⁷ U. Kerzel,²⁶ V. Khotilovich,⁵⁴ B. Kilminster,⁴⁰ D.H. Kim,²⁸ H.S. Kim,²⁸ J.E. Kim,²⁸ M.J. Kim,¹² S.B. Kim,²⁸ S.H. Kim,⁵⁶ Y.K. Kim,¹³ N. Kimura,⁵⁶ L. Kirsch,⁶ S. Klimenko,¹⁸ M. Klute,³³ B. Knuteson,³³ B.R. Ko,¹⁶ K. Kondo,⁵⁸ D.J. Kong,²⁸ J. Konigsberg,¹⁸ A. Korytov,¹⁸ A.V. Kotwal,¹⁶ A. Kovalev,⁴⁶ A.C. Kraan,⁴⁶ J. Kraus,²⁴ I. Kravchenko,³³ M. Kreps,²⁶ J. Kroll,⁴⁶ N. Krumnack,⁴ M. Kruse,¹⁶ V. Krutelyov,¹⁰ T. Kubo,⁵⁶ S. E. Kuhlmann,² T. Kuhr,²⁶ Y. Kusakabe,⁵⁸ S. Kwang,¹³ A.T. Laasanen,⁴⁹ S. Lai,³⁴ S. Lami,⁴⁷ S. Lammel,¹⁷ M. Lancaster,³¹ R.L. Lander,⁷ K. Lannon,⁴⁰ A. Lath,⁵³ G. Latino,⁴⁷ I. Lazzizzera,⁴⁴ T. LeCompte,² J. Lee,⁵⁰ J. Lee,²⁸ Y.J. Lee,²⁸ S.W. Lee,⁵⁴ R. Lefèvre,³ N. Leonardo,³³ S. Leone,⁴⁷ S. Levy,¹³ J.D. Lewis,¹⁷ C. Lin,⁶¹ C.S. Lin,¹⁷ M. Lindgren,¹⁷ E. Lipeles,⁹ A. Lister,⁷ D.O. Litvintsev,¹⁷ T. Liu,¹⁷ N.S. Lockyer,⁴⁶ A. Loginov,⁶¹ M. Loreti,⁴⁴ P. Loverre,⁵² R.-S. Lu,¹ D. Lucchesi,⁴⁴ P. Lujan,²⁹ P. Lukens,¹⁷ G. Lungu,¹⁸ L. Lyons,⁴³ J. Lys,²⁹ R. Lysak,¹⁴ E. Lytken,⁴⁹ P. Mack,²⁶ D. MacQueen,³⁴ R. Madrak,¹⁷ K. Maeshima,¹⁷ K. Makhoul,³³ T. Maki,²³ P. Maksimovic,²⁵ S. Malde,⁴³ G. Manca,³⁰ F. Margaroli,⁵ R. Marginean,¹⁷ C. Marino,²⁶ C.P. Marino,²⁴ A. Martin,⁶¹ M. Martin,²¹ V. Martin,²¹ M. Martínez,³ T. Maruyama,⁵⁶ P. Mastrandrea,⁵² T. Masubuchi,⁵⁶ H. Matsunaga,⁵⁶ M.E. Mattson,⁵⁹ R. Mazini,³⁴ P. Mazzanti,⁵ K.S. McFarland,⁵⁰ P. McIntyre,⁵⁴ R. McNulty,³⁰ A. Mehta,³⁰ P. Mehtala,²³ S. Menzemer,¹¹ A. Menzione,⁴⁷ P. Merkel,⁴⁹ C. Mesropian,⁵¹ A. Messina,³⁶ T. Miao,¹⁷ N. Miladinovic,⁶ J. Miles,³³ R. Miller,³⁶ C. Mills,¹⁰ M. Milnik,²⁶ A. Mitra,¹ G. Mitselmakher,¹⁸ A. Miyamoto,²⁷ S. Moed,²⁰ N. Moggi,⁵ B. Mohr,⁸ R. Moore,¹⁷ M. Morello,⁴⁷ P. Movilla Fernandez,²⁹ J. Mülmenstädt,²⁹ A. Mukherjee,¹⁷ Th. Muller,²⁶ R. Mumford,²⁵ P. Murat,¹⁷ J. Nachtman,¹⁷ A. Nagano,⁵⁶ J. Naganoma,⁵⁸ I. Nakano,⁴¹ A. Napier,⁵⁷ V. Necula,¹⁸ C. Neu,⁴⁶

M.S. Neubauer,⁹ J. Nielsen,²⁹ T. Nigmanov,⁴⁸ L. Nodulman,² O. Norniella,³ E. Nurse,³¹ S.H. Oh,¹⁶ Y.D. Oh,²⁸ I. Oksuzian,¹⁸ T. Okusawa,⁴² R. Oldeman,³⁰ R. Orava,²³ K. Osterberg,²³ C. Pagliarone,⁴⁷ E. Palencia,¹¹ V. Papadimitriou,¹⁷ A.A. Paramonov,¹³ B. Parks,⁴⁰ S. Pashapour,³⁴ J. Patrick,¹⁷ G. Pauletta,⁵⁵ M. Paulini,¹² C. Paus,³³ D.E. Pellett,⁷ A. Penzo,⁵⁵ T.J. Phillips,¹⁶ G. Piacentino,⁴⁷ J. Piedra,⁴⁵ L. Pinera,¹⁸ K. Pitts,²⁴ C. Plager,⁸ L. Pondrom,⁶⁰ X. Portell,³ O. Poukhov,¹⁵ N. Pounder,⁴³ F. Prakoshyn,¹⁵ A. Pronko,¹⁷ J. Proudfoot,² F. Ptohos^e,¹⁹ G. Punzi,⁴⁷ J. Pursley,²⁵ J. Rademacker^b,⁴³ A. Rahaman,⁴⁸ N. Ranjan,⁴⁹ S. Rappoccio,²² B. Reisert,¹⁷ V. Rekovic,³⁸ P. Renton,⁴³ M. Rescigno,⁵² S. Richter,²⁶ F. Rimondi,⁵ L. Ristori,⁴⁷ A. Robson,²¹ T. Rodrigo,¹¹ E. Rogers,²⁴ S. Rolli,⁵⁷ R. Roser,¹⁷ M. Rossi,⁵⁵ R. Rossin,¹⁸ A. Ruiz,¹¹ J. Russ,¹² V. Rusu,¹³ H. Saarikko,²³ S. Sabik,³⁴ A. Safonov,⁵⁴ W.K. Sakumoto,⁵⁰ G. Salamanna,⁵² O. Saltó,³ D. Saltzberg,⁸ C. Sánchez,³ L. Santi,⁵⁵ S. Sarkar,⁵² L. Sartori,⁴⁷ K. Sato,¹⁷ P. Savard,³⁴ A. Savoy-Navarro,⁴⁵ T. Scheidle,²⁶ P. Schlabach,¹⁷ E.E. Schmidt,¹⁷ M.P. Schmidt,⁶¹ M. Schmitt,³⁹ T. Schwarz,⁷ L. Scodellaro,¹¹ A.L. Scott,¹⁰ A. Scribano,⁴⁷ F. Scuri,⁴⁷ A. Sedov,⁴⁹ S. Seidel,³⁸ Y. Seiya,⁴² A. Semenov,¹⁵ L. Sexton-Kennedy,¹⁷ A. Sfyrta,²⁰ M.D. Shapiro,²⁹ T. Shears,³⁰ P.F. Shepard,⁴⁸ D. Sherman,²² M. Shimojima^k,⁵⁶ M. Shochet,¹³ Y. Shon,⁶⁰ I. Shreyber,³⁷ A. Sidoti,⁴⁷ P. Sinervo,³⁴ A. Sisakyan,¹⁵ J. Sjolin,⁴³ A.J. Slaughter,¹⁷ J. Slaunwhite,⁴⁰ K. Sliwa,⁵⁷ J.R. Smith,⁷ F.D. Snider,¹⁷ R. Snihur,³⁴ M. Soderberg,³⁵ A. Soha,⁷ S. Somalwar,⁵³ V. Sorin,³⁶ J. Spalding,¹⁷ F. Spinella,⁴⁷ T. Spreitzer,³⁴ P. Squillacioti,⁴⁷ M. Stanitzki,⁶¹ A. Staveris-Polykalas,⁴⁷ R. St. Denis,²¹ B. Stelzer,⁸ O. Stelzer-Chilton,⁴³ D. Stentz,³⁹ J. Strologas,³⁸ D. Stuart,¹⁰ J.S. Suh,²⁸ A. Sukhanov,¹⁸ H. Sun,⁵⁷ T. Suzuki,⁵⁶ A. Taffard,²⁴ R. Takashima,⁴¹ Y. Takeuchi,⁵⁶ K. Takikawa,⁵⁶ M. Tanaka,² R. Tanaka,⁴¹ M. Tecchio,³⁵ P.K. Teng,¹ K. Terashi,⁵¹ J. Thom^d,¹⁷ A.S. Thompson,²¹ E. Thomson,⁴⁶ P. Tipton,⁶¹ V. Tiwari,¹² S. Tkaczyk,¹⁷ D. Toback,⁵⁴ S. Tokar,¹⁴ K. Tollefson,³⁶ T. Tomura,⁵⁶ D. Tonelli,⁴⁷ S. Torre,¹⁹ D. Torretta,¹⁷ S. Tourneur,⁴⁵ W. Trischuk,³⁴ R. Tsuchiya,⁵⁸ S. Tsuno,⁴¹ N. Turini,⁴⁷ F. Ukegawa,⁵⁶ T. Unverhau,²¹ S. Uozumi,⁵⁶ D. Usynin,⁴⁶ S. Vallecorsa,²⁰ N. van Remortel,²³ A. Varganov,³⁵ E. Vataga,³⁸ F. Vázquezⁱ,¹⁸ G. Velev,¹⁷ G. Veramendi,²⁴ V. Veszpremi,⁴⁹ R. Vidal,¹⁷ I. Vila,¹¹ R. Vilar,¹¹ T. Vine,³¹ I. Vollrath,³⁴ I. Volobouevⁿ,²⁹ G. Volpi,⁴⁷ F. Würthwein,⁹ P. Wagner,⁵⁴ R.G. Wagner,² R.L. Wagner,¹⁷ J. Wagner,²⁶ W. Wagner,²⁶ R. Wallny,⁸ S.M. Wang,¹ A. Warburton,³⁴ S. Waschke,²¹ D. Waters,³¹ M. Weinberger,⁵⁴ W.C. Wester III,¹⁷ B. Whitehouse,⁵⁷ D. Whiteson,⁴⁶ A.B. Wicklund,² E. Wicklund,¹⁷ G. Williams,³⁴ H.H. Williams,⁴⁶ P. Wilson,¹⁷ B.L. Winer,⁴⁰ P. Wittich^d,¹⁷ S. Wolbers,¹⁷ C. Wolfe,¹³ T. Wright,³⁵ X. Wu,²⁰ S.M. Wynne,³⁰ A. Yagil,¹⁷ K. Yamamoto,⁴² J. Yamaoka,⁵³ T. Yamashita,⁴¹ C. Yang,⁶¹ U.K. Yang^j,¹³ Y.C. Yang,²⁸ W.M. Yao,²⁹ G.P. Yeh,¹⁷ J. Yoh,¹⁷ K. Yorita,¹³ T. Yoshida,⁴² G.B. Yu,⁵⁰ I. Yu,²⁸ S.S. Yu,¹⁷ J.C. Yun,¹⁷ L. Zanello,⁵² A. Zanetti,⁵⁵ I. Zaw,²² X. Zhang,²⁴ J. Zhou,⁵³ and S. Zucchelli⁵

(CDF Collaboration*)

¹*Institute of Physics, Academia Sinica, Taipei, Taiwan 11529, Republic of China*

²*Argonne National Laboratory, Argonne, Illinois 60439*

³*Institut de Física d'Altes Energies, Universitat Autònoma de Barcelona, E-08193, Bellaterra (Barcelona), Spain*

⁴*Baylor University, Waco, Texas 76798*

⁵*Istituto Nazionale di Fisica Nucleare, University of Bologna, I-40127 Bologna, Italy*

⁶*Brandeis University, Waltham, Massachusetts 02254*

⁷*University of California, Davis, Davis, California 95616*

⁸*University of California, Los Angeles, Los Angeles, California 90024*

⁹*University of California, San Diego, La Jolla, California 92093*

¹⁰*University of California, Santa Barbara, Santa Barbara, California 93106*

¹¹*Instituto de Física de Cantabria, CSIC-University of Cantabria, 39005 Santander, Spain*

¹²*Carnegie Mellon University, Pittsburgh, PA 15213*

¹³*Enrico Fermi Institute, University of Chicago, Chicago, Illinois 60637*

¹⁴*Comenius University, 842 48 Bratislava, Slovakia; Institute of Experimental Physics, 040 01 Kosice, Slovakia*

¹⁵*Joint Institute for Nuclear Research, RU-141980 Dubna, Russia*

¹⁶*Duke University, Durham, North Carolina 27708*

¹⁷*Fermi National Accelerator Laboratory, Batavia, Illinois 60510*

¹⁸*University of Florida, Gainesville, Florida 32611*

¹⁹*Laboratori Nazionali di Frascati, Istituto Nazionale di Fisica Nucleare, I-00044 Frascati, Italy*

²⁰*University of Geneva, CH-1211 Geneva 4, Switzerland*

²¹*Glasgow University, Glasgow G12 8QQ, United Kingdom*

²²*Harvard University, Cambridge, Massachusetts 02138*

²³*Division of High Energy Physics, Department of Physics,*

University of Helsinki and Helsinki Institute of Physics, FIN-00014, Helsinki, Finland

²⁴*University of Illinois, Urbana, Illinois 61801*

²⁵*The Johns Hopkins University, Baltimore, Maryland 21218*

²⁶*Institut für Experimentelle Kernphysik, Universität Karlsruhe, 76128 Karlsruhe, Germany*

²⁷*High Energy Accelerator Research Organization (KEK), Tsukuba, Ibaraki 305, Japan*

- ²⁸Center for High Energy Physics: Kyungpook National University, Taegu 702-701, Korea; Seoul National University, Seoul 151-742, Korea; and SungKyunKwan University, Suwon 440-746, Korea
- ²⁹Ernest Orlando Lawrence Berkeley National Laboratory, Berkeley, California 94720
- ³⁰University of Liverpool, Liverpool L69 7ZE, United Kingdom
- ³¹University College London, London WC1E 6BT, United Kingdom
- ³²Centro de Investigaciones Energeticas Medioambientales y Tecnologicas, E-28040 Madrid, Spain
- ³³Massachusetts Institute of Technology, Cambridge, Massachusetts 02139
- ³⁴Institute of Particle Physics: McGill University, Montréal, Canada H3A 2T8; and University of Toronto, Toronto, Canada M5S 1A7
- ³⁵University of Michigan, Ann Arbor, Michigan 48109
- ³⁶Michigan State University, East Lansing, Michigan 48824
- ³⁷Institution for Theoretical and Experimental Physics, ITEP, Moscow 117259, Russia
- ³⁸University of New Mexico, Albuquerque, New Mexico 87131
- ³⁹Northwestern University, Evanston, Illinois 60208
- ⁴⁰The Ohio State University, Columbus, Ohio 43210
- ⁴¹Okayama University, Okayama 700-8530, Japan
- ⁴²Osaka City University, Osaka 588, Japan
- ⁴³University of Oxford, Oxford OX1 3RH, United Kingdom
- ⁴⁴University of Padova, Istituto Nazionale di Fisica Nucleare, Sezione di Padova-Trento, I-35131 Padova, Italy
- ⁴⁵LPNHE, Universite Pierre et Marie Curie/IN2P3-CNRS, UMR7585, Paris, F-75252 France
- ⁴⁶University of Pennsylvania, Philadelphia, Pennsylvania 19104
- ⁴⁷Istituto Nazionale di Fisica Nucleare Pisa, Universities of Pisa, Siena and Scuola Normale Superiore, I-56127 Pisa, Italy
- ⁴⁸University of Pittsburgh, Pittsburgh, Pennsylvania 15260
- ⁴⁹Purdue University, West Lafayette, Indiana 47907
- ⁵⁰University of Rochester, Rochester, New York 14627
- ⁵¹The Rockefeller University, New York, New York 10021
- ⁵²Istituto Nazionale di Fisica Nucleare, Sezione di Roma 1, University of Rome "La Sapienza," I-00185 Roma, Italy
- ⁵³Rutgers University, Piscataway, New Jersey 08855
- ⁵⁴Texas A&M University, College Station, Texas 77843
- ⁵⁵Istituto Nazionale di Fisica Nucleare, University of Trieste/ Udine, Italy
- ⁵⁶University of Tsukuba, Tsukuba, Ibaraki 305, Japan
- ⁵⁷Tufts University, Medford, Massachusetts 02155
- ⁵⁸Waseda University, Tokyo 169, Japan
- ⁵⁹Wayne State University, Detroit, Michigan 48201
- ⁶⁰University of Wisconsin, Madison, Wisconsin 53706
- ⁶¹Yale University, New Haven, Connecticut 06520

(Dated: December 22, 2006)

We report a measurement of the ratio of branching fractions of the decays $B^\pm \rightarrow J/\psi\pi^\pm$ and $B^\pm \rightarrow J/\psi K^\pm$ using the CDF II detector at the Fermilab Tevatron Collider. The signal from the Cabibbo-suppressed $B^\pm \rightarrow J/\psi\pi^\pm$ decay is separated from $B^\pm \rightarrow J/\psi K^\pm$ using the $B^\pm \rightarrow J/\psi K^\pm$ invariant mass distribution and the kinematical differences of the hadron track in the two decay modes. From a sample of 220 pb⁻¹ of $p\bar{p}$ collisions at $\sqrt{s} = 1.96$ TeV, we observe 91 ± 15 $B^\pm \rightarrow J/\psi\pi^\pm$ events together with 1883 ± 34 $B^\pm \rightarrow J/\psi K^\pm$ events. The ratio of branching fractions is found to be $\mathcal{B}(B^\pm \rightarrow J/\psi\pi^\pm)/\mathcal{B}(B^\pm \rightarrow J/\psi K^\pm) = (4.86 \pm 0.82(\text{stat.}) \pm 0.15(\text{syst.}))\%$.

PACS numbers: 13.25.Hw 14.40.Nd

*With visitors from ^aUniversity of Athens, ^bUniversity of Bristol, ^cUniversity Libre de Bruxelles, ^dCornell University, ^eUniversity of Cyprus, ^fUniversity of Dublin, ^gUniversity of Edinburgh, ^hUniversity of Heidelberg, ⁱUniversidad Iberoamericana, ^jUniversity of Manchester, ^kNagasaki Institute of Applied Science, ^lUniversity de Oviedo, ^mUniversity of London, Queen Mary and Westfield College, ⁿTexas Tech University, ^oIFIC(CSIC-Universitat de Valencia),

The $B^\pm \rightarrow J/\psi\pi^\pm$ decay is a Cabibbo-suppressed mode proceeding via a $b \rightarrow c\bar{c}d$ transition. If the leading-order tree diagram is the dominant contribution, its branching fraction is expected to be $\approx 5\%$ of that of the Cabibbo-favored mode $B^\pm \rightarrow J/\psi K^\pm$. Detailed predictions of the ratio are obtained using the hypothesis of factorization of the hadronic matrix elements [1, 2], a theoretical approach widely used in the treatment of non-leptonic decays of B mesons. However, the absence of strong theoretical arguments supporting factorization and the use of phenomenological models,

which are a source of theoretical uncertainties, weakens the reliability of those predictions, which need to be accurately tested on data. Until now, the measurements on the $B^\pm \rightarrow J/\psi\pi^\pm$ decay were performed by many experiments. The BABAR collaboration reported $\mathcal{B}(B^\pm \rightarrow J/\psi\pi^\pm)/\mathcal{B}(B^\pm \rightarrow J/\psi K^\pm) = (5.37 \pm 0.45)\%$ with 244 ± 20 $B^\pm \rightarrow J/\psi\pi^\pm$ events [3]. The Belle collaboration reported $\mathcal{B}(B^\pm \rightarrow J/\psi\pi^\pm) = (3.8 \pm 0.6) \times 10^{-5}$ [4]. A previous study of the $B^\pm \rightarrow J/\psi\pi^\pm$ decay was also performed by the CLEO collaboration [5]. The result of this analysis supersedes the previous CDF result [6].

This paper presents a measurement of the ratio of branching fractions $\mathcal{B}(B^\pm \rightarrow J/\psi\pi^\pm)/\mathcal{B}(B^\pm \rightarrow J/\psi K^\pm)$. We use a sample of fully reconstructed $B^\pm \rightarrow J/\psi K^\pm$ decays, where $J/\psi \rightarrow \mu^+\mu^-$, corresponding to an integrated luminosity of 220 pb^{-1} of $p\bar{p}$ collisions at $\sqrt{s} = 1.96 \text{ TeV}$ collected by the CDF II detector at Fermilab between February 2002 and August 2003.

The CDF II detector is a multipurpose detector [7] with a central geometry and has a tracking system surrounded by calorimeters and muon detectors. The components of the detector most relevant to this analysis are described briefly here. Charged particle trajectories are reconstructed in the pseudorapidity range $|\eta| < 1.0$, where $\eta = -\ln(\tan \frac{\theta}{2})$ and θ is the polar angle measured from the beam line [8]. Trajectories are reconstructed from hits in the silicon microstrip detector (SVX II) [9] and the central outer tracker (COT) [10] which are immersed in a 1.4 T solenoidal magnetic field. The SVX II consists of five concentric layers made of double-sided silicon detectors with radii between 2.5 and 10.6 cm, each providing a position measurement with $15 \mu\text{m}$ resolution in the r - ϕ plane. The COT is an open-cell drift chamber with 96 measurement layers, between 40 and 137 cm in radius, organized into eight alternating axial and $\pm 2^\circ$ stereo superlayers. The transverse momentum (p_T) resolution is $\sigma_{p_T}/p_T \simeq 0.15\% p_T (\text{GeV}/c)^{-1}$. Muon detectors consisting of multi-layer drift chambers are located radially around the outside of the calorimeter [11]. The central muon detector (CMU) covers a range in pseudorapidity of $|\eta| < 0.6$. The central muon extension (CMX) extends the pseudorapidity coverage to $0.6 < |\eta| < 1.0$.

The data sample used in this analysis required a dimuon trigger sensitive to $J/\psi \rightarrow \mu^+\mu^-$. The CDF II detector employs a three-level trigger system to select events of interest efficiently. At the first trigger level, muon candidates are identified by matching track segments in the CMU and CMX to coarsely reconstructed COT tracks obtained with the extremely fast tracker (XFT) [12]. Dimuon triggers use combinations of CMU-CMU and CMU-CMX muons with $p_T > 1.5$ (2.0) GeV/c for CMU (CMX) muons. For the data presented here, no additional requirements are made at the second level. At the third trigger level, a detailed reconstruction is performed and oppositely charged dimuon events with an invariant mass in the range of $2.7 - 4.0 \text{ GeV}/c^2$ are selected.

In this analysis, we reconstruct $B^\pm \rightarrow J/\psi K^\pm$ de-

cays. B meson decay modes involving the well-known $J/\psi \rightarrow \mu^+\mu^-$ decay have been extensively used in other measurements at CDF, and their selection criteria are well established. We follow the selection requirements developed in the b hadron mass measurement [13] and apply them to the B^\pm decay mode of interest.

The $B^\pm \rightarrow J/\psi K^\pm$ reconstruction begins by selecting $J/\psi \rightarrow \mu^+\mu^-$ candidates with pairs of oppositely charged tracks which satisfy the requirements of the dimuon triggers. J/ψ candidates are further selected by requiring their invariant mass to be within $80 \text{ MeV}/c^2$ of the world average J/ψ mass [14]. After a J/ψ candidate is identified, any other charged track is assumed to be a kaon and is combined with the J/ψ candidate to make a B^\pm candidate. The tracks of the kaon and two muons are then fitted to a common three dimensional vertex (3-D) while constraining the invariant mass of two muons to the world average J/ψ mass [14]. To ensure good vertex resolution, each track must have hits in at least three silicon vertex detector layers in the $r - \phi$ plane and the probability resulting from the 3-D vertex fit is required to be greater than 1%.

A number of further requirements are made to improve the signal-to-background separation. Prompt background, with tracks coming directly from the primary vertex, can be reduced by exploiting variables sensitive to the long lifetime of the B^\pm meson. To reduce prompt background, the transverse decay length (L_{xy}) of the B^\pm is required to exceed $200 \mu\text{m}$, where L_{xy} is defined as the vector from the primary vertex to the B^\pm decay vertex projected onto the p_T of the B^\pm candidate. To further reduce combinatorial background, we require $p_T > 6.5 \text{ GeV}/c$ for the B^\pm candidate and $p_T > 2.0 \text{ GeV}/c$ for the hadron from the B^\pm decay. The values used in the above selection criteria are determined by an iterative optimization procedure in which the significance $S/\sqrt{S+B}$ is maximized. The quantity S represents the number of accepted signal events, in this case taken from a Monte Carlo simulation sample, and B is the number of selected B^\pm candidates within the mass sidebands of the data.

We measure the following ratio:

$$\begin{aligned} \frac{\mathcal{B}(B^\pm \rightarrow J/\psi\pi^\pm)}{\mathcal{B}(B^\pm \rightarrow J/\psi K^\pm)} &= \frac{N_{J/\psi\pi^\pm}}{N_{J/\psi K^\pm}} \times \frac{\epsilon_{J/\psi K^\pm}}{\epsilon_{J/\psi\pi^\pm}} \\ &= r_{obs} \times \frac{1}{\epsilon_{rel}}, \end{aligned} \quad (1)$$

where $r_{obs} (\equiv N_{J/\psi\pi^\pm}/N_{J/\psi K^\pm})$ is the ratio of the yields of each decay mode, and $\epsilon_{rel} (\equiv \epsilon_{J/\psi\pi^\pm}/\epsilon_{J/\psi K^\pm})$ is the relative reconstruction efficiency. In this analysis, the quantity r_{obs} is extracted from an unbinned maximum likelihood fit using the differences between the two decay modes in the mass distribution, and is corrected with ϵ_{rel} obtained from Monte Carlo simulation.

To build the probability density function (PDF) used in the unbinned maximum likelihood fit, we choose the invariant mass of two muons and a kaon ($M_{\mu\mu K}$) as an

observable. There are three components in the distribution of the $M_{\mu\mu K}$ variable: the $B^\pm \rightarrow J/\psi K^\pm$ signal, the $B^\pm \rightarrow J/\psi\pi^\pm$ signal and the combinatorial background. We model the $B^\pm \rightarrow J/\psi K^\pm$ signal as a Gaussian centered at the mass of B^\pm (M_B) with a width σ_K . If the pion mass were assigned to the hadron track originating from the $B^\pm \rightarrow J/\psi\pi^\pm$ decay, the resulting spectrum would be also a Gaussian centered at M_B . However, assigning the kaon mass to this track produces a spectrum partially overlapping the $B^\pm \rightarrow J/\psi K^\pm$ and shifted in the positive direction. The shifted invariant mass of $B^\pm \rightarrow J/\psi\pi^\pm$ can be calculated by an approximation, which has a good agreement with the exact value,

$$\mathcal{M}'_B(\alpha) \simeq M_B^2 + (1 + \alpha)(M_K^2 - M_\pi^2), \quad (2)$$

where M_K and M_π are respectively the kaon and the pion masses. The purely kinematic variable α is defined as $\alpha \equiv E_{J/\psi}/P_K$, where $E_{J/\psi}$ is the J/ψ energy and P_K is the magnitude of the momentum of the hadron track. Using Eq. (2), the $B^\pm \rightarrow J/\psi\pi^\pm$ signal is modeled as a Gaussian centered at $\mathcal{M}'_B(\alpha)$ with a width σ_π . We find σ_K and σ_π have almost the same value from the Monte Carlo simulation, so we constrain them to be the same value in the fit to reduce the systematic uncertainty. We assume the background mass distribution is a first order polynomial. Since α is slightly correlated with $M_{\mu\mu K}$, it is chosen as another observable in the likelihood. To model the α distributions of the two signals, we param-

eterize them from Monte Carlo simulation. We also parameterize the α distribution of the background, which is obtained from the mass sidebands of the data. These mass sidebands are chosen from $5.2 < M_{\mu\mu K} < 5.24$ and $5.4 < M_{\mu\mu K} < 5.6$ GeV/c^2 to avoid signal contaminations and other backgrounds from partially reconstructed B mesons that fall below 5.2 GeV/c^2 . The empirical functions used in the parameterizations are

$$h_{J/\psi X}(\alpha; f_i, \lambda_i, a) = \sum_{i=1}^3 f_i(\alpha - a)e^{-\lambda_i \alpha} \quad (3)$$

$$h_{bkg}(\alpha; f_i, \lambda_i, a) = \sum_{i=1}^3 f_i(\alpha - a)^3 e^{-\lambda_i \alpha}, \quad (4)$$

where the symbol X denotes K or π in Eq. (3) and f_1 , f_2 and f_3 are to be the fractional contributions of each type of function when the functions are properly normalized to 1. Because of the requirement on the p_T of the hadron track and also of the dimuon triggers, all α distributions show a cutoff around 0.5 in the α variable and these cutoff values are parameterized by a in Eq. (3) and (4). These parameters of the functions describing the α distributions are fixed in the fit. The α distributions of the signal and background, and the results of the parameters are shown in Fig. 1. With models for each signal and background, and with the chosen observables, the PDF of the i^{th} event is written as

$$p_i = f_s \left[\frac{1}{1 + r_{obs}} G(M_{\mu\mu K}^i - M_B, \sigma) h_{J/\psi K}(\alpha^i) + \frac{r_{obs}}{1 + r_{obs}} G(M_{\mu\mu K}^i - \mathcal{M}'_B(\alpha^i), \sigma) h_{J/\psi\pi}(\alpha^i) \right] + (1 - f_s) B(M_{\mu\mu K}^i) h_{bkg}(\alpha^i), \quad (5)$$

where f_s is the fraction of signal events in the data sample and r_{obs} is the ratio between the yields of each signal. The functions, $G(M_{\mu\mu K}^i - M_B, \sigma)$ and $G(M_{\mu\mu K}^i - \mathcal{M}'_B(\alpha^i), \sigma)$, are Gaussians with a width σ describing the mass distributions of $B^\pm \rightarrow J/\psi K^\pm$ and $B^\pm \rightarrow J/\psi\pi^\pm$, respectively, and $B(M_{\mu\mu K}^i)$ is a first order polynomial function which describes the background mass distribution. The fitting range ($5.2 < M_{\mu\mu K} < 5.6$ GeV/c^2) is carefully selected to avoid the backgrounds from partially reconstructed B mesons, but to include enough of the background region to determine accurately the background shape. $\mathcal{L} = \prod_{i=1}^N p_i$ is then maximized to obtain the best fit values for M_B , σ , f_s and r_{obs} .

The fit to 2683 candidates falling in the fitting range returns the signal fraction, $f_s = 0.736 \pm 0.012$, and the ratio of the yields of each decay mode, $r_{obs} = (4.82 \pm 0.81)\%$. These values give 1883 ± 34 signal events in the $B^\pm \rightarrow J/\psi K^\pm$ decay mode and 91 ± 15 events in the

$B^\pm \rightarrow J/\psi\pi^\pm$ decay mode. The distributions in $M_{\mu\mu K}$ and α for the events in the data sample are shown in Fig. 2 and Fig. 3, along with the likelihood fit results.

Possible biases in the fitting procedure are investigated by performing the fit on samples generated by the PDF in Eq. (5), with known composition and with the same size as the data sample. The difference of the ratio between the extracted and the input values is consistent with zero and the width of the pull distributions is one.

In order to determine the ratio of branching fractions, the ratio of the yields of each decay mode must be corrected with the relative reconstruction efficiency. The relative reconstruction efficiency depends in turn on the different decay-in-flights and nuclear interaction probabilities of the kaon and pion from the two decay modes and on the slightly different track momentum spectra. The relative reconstruction efficiency for the two decay modes is $\epsilon_{rel} = 0.991 \pm 0.005$ which is derived from the Monte Carlo simulation.

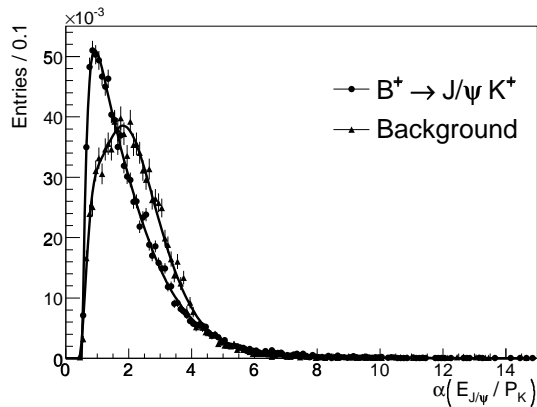


FIG. 1: The α distributions of $B^\pm \rightarrow J/\psi K^\pm$, which are obtained with Monte Carlo simulation, and background obtained from the non-signal data sample. The solid curves are the corresponding parameterization functions from Eq. (3) and (4). The α distributions of the two signals are very similar in shape due to the almost identical kinematics of the two decay modes. To avoid confusion from it, we plot the α distribution of $B^\pm \rightarrow J/\psi K^\pm$ only.

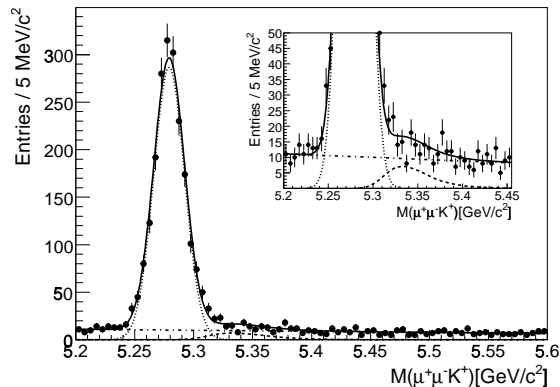


FIG. 2: The invariant mass distribution in the data sample (points) projected with the results of the likelihood fit; overall (solid line), $B^\pm \rightarrow J/\psi K^\pm$ (dotted line), $B^\pm \rightarrow J/\psi \pi^\pm$ (dashed line) and background (dashed-dotted line). The inset shows the magnified region of the $B^\pm \rightarrow J/\psi \pi^\pm$ signal.

In this analysis, we use a Monte Carlo simulation to parameterize the α distributions of each signal and to determine the relative reconstruction efficiency for the two decay modes. The Monte Carlo generation proceeds as follows. Transverse momentum and rapidity distributions of single b quarks are generated based on next-to-leading order (NLO) perturbative QCD calculation [15]. B meson kinematic distributions are obtained by simulating Peterson fragmentation [16] on quark-level distributions. Additional fragmentation particles, correlated $b\bar{b}$ production and the underlying event structure are not generated. The B meson spectrum used in the Monte

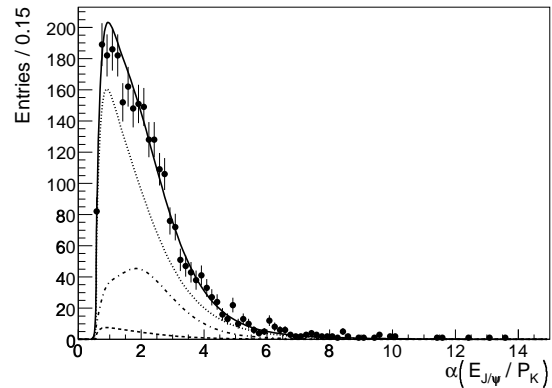


FIG. 3: The α distribution in the data sample (points) compared with the results of the likelihood fit; overall (solid line), $B^\pm \rightarrow J/\psi K^\pm$ (dotted line), $B^\pm \rightarrow J/\psi \pi^\pm$ (dashed line) and background (dashed-dotted line).

Carlo simulation is consistent with the data from inclusive $B \rightarrow J/\psi X$ [7]. The CLEOMC program [17] is used to decay B^\pm mesons into the final states of interest. The simulation of the CDF II detector and trigger is based on a GEANT [18] description.

Since both decay modes of interest have almost identical decay topology and kinematics, most systematic uncertainties cancel in this ratio measurement, including uncertainties in total integrated luminosity and trigger and reconstruction efficiencies. Remaining systematic uncertainties come from the uncertainties in the shapes of the mass distribution, the parameterized PDFs in the α variable, and from the determination of the relative reconstruction efficiency. The largest systematic uncertainty originates from the unknown shape of the combinatorial background in the mass distribution. To estimate this effect, a second order polynomial function is considered as an alternative model for the shape of the background mass distribution. The non-Gaussian tails in the mass distribution of $B^\pm \rightarrow J/\psi K^\pm$ can mimic the $B^\pm \rightarrow J/\psi \pi^\pm$ signal, which affects the ratio of the yields of each signal. We replace a Gaussian with a double Gaussian for modeling each signal mass distribution and fit again to evaluate the uncertainty coming from the non-Gaussian tails in the $B^\pm \rightarrow J/\psi K^\pm$ mass distribution. The uncertainties in the function parameters describing the PDFs in the α variable, in Eq. (3) and (4), generate an uncertainty for the ratio measurement. The contribution of this uncertainty is estimated by performing the fit by varying the parameters of the PDFs by $\pm 1\sigma$. The uncertainty in ϵ_{rel} originates from the uncertainties of the nuclear interaction and the material description in the detector simulation. The GEANT simulation calculates nuclear interaction probabilities of $\approx 4\%$ for π^+ , π^- and K^- , and $\approx 3\%$ for K^+ . We then assign a 25% uncertainty to the calculated nuclear interaction probabilities as the uncertainty of the detector

material description in the detector simulation, and take the resulting uncertainty in ϵ_{rel} as a systematic uncertainty. We determine the total systematic uncertainty of 3.0% on the measurement by adding the individual uncertainties in quadrature, and the contributions from each source are summarized in Table I.

TABLE I: Summary of systematic uncertainties for the ratio of branching fractions, $\mathcal{B}(B^\pm \rightarrow J/\psi\pi^\pm)/\mathcal{B}(B^\pm \rightarrow J/\psi K^\pm)$.

Source	Uncertainty of the ratio (%)
Background Shape	2.5
Non-Gaussian tail of $B^\pm \rightarrow J/\psi K^\pm$	1.2
α PDFs Parametrization	1.0
Relative Reconstruction Efficiency	0.5
Total Uncertainty	3.0

From Eq. (1), we derived the ratio of branching fractions,

$$\frac{\mathcal{B}(B^\pm \rightarrow J/\psi\pi^\pm)}{\mathcal{B}(B^\pm \rightarrow J/\psi K^\pm)} = (4.86 \pm 0.82(\text{stat.}) \pm 0.15(\text{syst.}))\%,$$

where the first error is statistical and the second is sys-

tematic.

In conclusion, we present the measurement of the ratio of branching fractions between $B^\pm \rightarrow J/\psi\pi^\pm$ and $B^\pm \rightarrow J/\psi K^\pm$. This result is consistent with theoretical expectations and the previous measurements, and will improve the present world average (5.3 ± 0.4)% [14].

We thank the Fermilab staff and the technical staffs of the participating institutions for their vital contributions. This work was supported by the U.S. Department of Energy and National Science Foundation; the Italian Istituto Nazionale di Fisica Nucleare; the Ministry of Education, Culture, Sports, Science and Technology of Japan; the Natural Sciences and Engineering Research Council of Canada; the National Science Council of the Republic of China; the Swiss National Science Foundation; the A.P. Sloan Foundation; the Bundesministerium für Bildung und Forschung, Germany; the Korean Science and Engineering Foundation and the Korean Research Foundation; the Particle Physics and Astronomy Research Council and the Royal Society, UK; the Russian Foundation for Basic Research; the Comisión Interministerial de Ciencia y Tecnología, Spain; in part by the European Community's Human Potential Programme under contract HPRN-CT-2002-00292; and the Academy of Finland.

-
- [1] M. Wirbel, B. Stech, and M. Bauer, Phys. C **24**, 637 (1985).
- [2] M. Bauer, B. Stech, and M. Wirbel, Phys. C **34**, 103 (1987).
- [3] B. Aubert *et al.* (BaBar Collaboration), Phys. Rev. Lett. **92**, 241802 (2004).
- [4] K. Abe *et al.* (Belle Collaboration), Phys. Rev. D **67**, 032003 (2003).
- [5] M. Bishai *et al.* (CLEO Collaboration), Phys. Lett. B **369**, 189 (1996).
- [6] F. Abe *et al.* (CDF Collaboration), Phys. Rev. Lett. **77**, 5176 (1996).
- [7] D. Acosta *et al.* (CDF Collaboration), Phys. Rev. D **71**, 032001 (2005).
- [8] CDF II uses a cylindrical coordinate system in which ϕ is the azimuthal angle, r is the radius from the nominal beam line, and z points in the beam direction, with the origin at the center of the detector. The $r - \phi$ plane is the transverse plane perpendicular to the z axis.
- [9] A. Sill *et al.*, Nucl. Instrum. Methods A **447**, 1 (2000).
- [10] T. Affolder *et al.*, Nucl. Instrum. Methods A **526**, 249 (2004).
- [11] G. Ascoli *et al.*, Nucl. Instrum. Methods A **268**, 33 (1998).
- [12] E. J. Thomson *et al.*, IEEE Trans. Nucl. Sci. **49**, 1063 (2002).
- [13] D. Acosta *et al.* (CDF Collaboration), hep-ex/0508022, submitted to PRL
- [14] The Particle Data Group, S. Eidelman *et al.*, Phys. Lett. B **592**, 1 (2004).
- [15] P. Nason, S. Dawson, and R. K. Ellis, Nucl. Phys. B **303**, 607 (1998).
- [16] C. Peterson *et al.*, Phys. Rev. D **27**, 105 (1983).
- [17] P. Avery, K. Read, and G. Trahern, Cornell internal Note CSN-212, 1985 (unpublished).
- [18] R. Brun, R. Hagelberg, M. Hansroul, and J.C. Lassalle, CERN Report No. CERN-DD-78-2-REV (1987); CERN Report No. CERN-DD-78-2 (1987).